International Journal of Pressure Vessels and Piping 212 (2024) 105303

Contents lists available at ScienceDirect

International Journal of Pressure Vessels and Piping

journal homepage: www.elsevier.com/locate/ijpvp

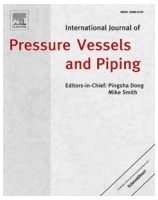

Detection of deposits adhered on the back surface of plate-like structures using a scanning laser source technique

Shoma Tanaka, Takahiro Hayashi *, Naoki Mori

Department of Mechanical Engineering, Graduate School of Engineering, Osaka University, Suita, Osaka 565-0871, Japan

A B S T R A C T

An imaging technique using a scanning laser source (SLS) was applied to detect deposits inside pipes, which are necessary for the safe decommissioning of the Fukushima Nuclear Power Plant. Experimental results showed that the more firmly adhered the deposit on the back surface of a flat plate, the clearer it is to obtain an image of the deposit. This result is as expected because the imaging by an SLS technique is dependent on the bending stiffness of the thin plate structure. Furthermore, even epoxy putty as large as 50 mm in diameter adhered to the inner surface of the pipe could be imaged, and even when the receiver device was changed from a piezoelectric device to a non-contact laser doppler vibrometer, the image of the deposit could be obtained properly with some degradation of the image due to the effect of a lower signal-to-noise ratio.

1. Introduction

Numerous pipes in chemical, thermal, and nuclear power plants play a very important role in transporting liquids, gases, and slurries. These pipes are subjected to erosion and corrosion, and to various loads from the external environment, and in some locations, extremely severe fatigue can accumulate. Therefore, piping inspections are performed on a regular basis, and various piping inspection methods are applied according to the inspection target [1,2].

Radiographic and ultrasonic testing are commonly used for pipe inspection. Radiographic inspection is a very effective means of obtaining fluoroscopic images of the inside of pipes, but it requires a thorough knowledge of radiation for safe handling. On the other hand, ultrasonics, which is also used to obtain images of the inside of the human body, has no major safety hazards and is very easy to handle in the development of new techniques. However, all of these methods require probes and measuring devices to be mounted close to the pipe to be inspected, and workers must climb up to the target pipe on scaffolding and then approach it for inspection. This is one of the main factors that increase the burden of pipe inspection.

Therefore, research and development has been conducted on guided wave inspection, in which an ultrasonic mode called a guided wave is propagated in the longitudinal and circumferential directions of a pipe for efficient inspection, and it was put into practical use in the 2000's [3–10]. However, it is necessary to use a low-frequency range having low attenuation for long-distance inspection, and the resolution of defect detection is limited by the diffraction limit, making it impossible to detect defects of the desired size. For this reason, the authors have studied a remote defect imaging method using a scanning laser source (SLS) technique [11–20]. This method utilizes the fact that the vibration energy generated by laser irradiation depends on the bending stiffness of the area near the irradiated point. Therefore, its defect detection resolution is independent of the diffraction limit of the pulse echo method, and it also has the advantage that defects can be detected by remote measurement.

The ultimate goal of this research is to apply this imaging technique to the evaluation of deposits in pipes and to contribute to the decommissioning of the Fukushima Daiichi Nuclear Power Plant. The Fukushima Daiichi Nuclear Power Plant lost its power supply due to the tsunami that struck in March 2011, and as a result, important safety functions such as water injection to the reactors and condition monitoring were lost. Units 1–3, which were in operation, experienced meltdowns, and Unit 4 experienced a hydrogen explosion during routine inspections. Currently, the decommissioning of all Units 1–6 is underway [21]. In the decommissioning process, before removing the fuel debris and dismantling the reactor buildings and pressure vessels, the removal of unneeded piping in the surrounding areas is also a major workload. This is because the piping of the Fukushima Daiichi Nuclear Power Plant, which was shut down by the tsunami, may contain various kinds of deposits including radioactive materials. Therefore, we must carefully remove while confirming their presence [22]. Since some areas around these pipes have high radiation level, the detection of internal deposits should be done remotely, if possible, to ensure the safety of workers with limited cumulative exposure doses, and an imaging

* Corresponding author.
E-mail address: hayashi@mech.eng.osaka-u.ac.jp (T. Hayashi).

https://doi.org/10.1016/j.ijpvp.2024.105303
Received 24 April 2024; Received in revised form 21 August 2024; Accepted 30 August 2024
Available online 3 September 2024

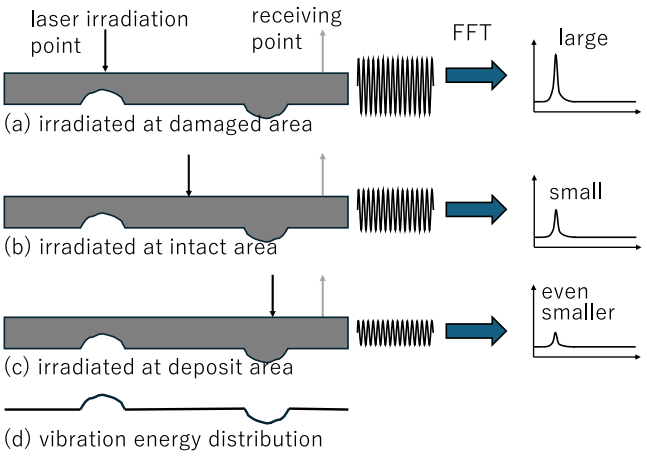

Fig. 1. Differences of vibration energy depending on the plate thickness at laser irradiation points.

method using an SLS technique meets this need.

With the above background, this study attempts to apply an SLS technique to objects adhering to the backside of thin objects. First, basic experiments are conducted on a solid piece adhered to a flat aluminum plate, and then a deposit in a pipe is visualized.

2. Imaging principle using an SLS technique

Before describing the evaluation of deposits, the principle of imaging the back surface of plate-like structures using an SLS is explained. When a laser is instantaneously irradiated onto a metallic material, elastic waves are generated due to the effects of thermo-elasticity and ablation [23–26]. Generally, when the laser output power is high, ablation of the material surface generates ultrasonic waves. When the laser power is low enough not to cause ablation, ultrasonic waves are generated due to the thermo-elastic effect. In this study, experiments were conducted using laser power at which only the thermo-elastic effect occurs so as not to damage the material surface.

When a laser is instantaneously irradiated onto the surface of a plate-like structure, a low-frequency antisymmetric mode of Lamb wave, generally called A0 mode, is generated with bending vibration [26]. In previous studies by the authors [11–20], damage to the back surface of a thin plate and wall thinning on the inner surface of a pipe were imaged using the phenomenon that the bending stiffness varies with the plate thickness at the laser irradiation point and the bending vibration energy generated changes accordingly. Here, the decrease in vibration energy caused by the increase in bending stiffness due to deposits is imaged. Fig. 1 shows a schematic diagram of the principle. If the laser irradiation point is directly above the damaged area where the plate thickness is thinner, the flexural vibrations generated will be large because the bending rigidity is smaller (Fig. 1 (a)). On the other hand, if the laser irradiation point is on a thicker plate, the flexural vibrations generated are smaller due to the higher bending rigidity (Fig. 1 (b)). If the laser irradiated point is a thicker plate with a deposit the flexural vibration generated will be even smaller due to the greater bending rigidity (Fig. 1 (c)). In this study, based on this prediction, imaging of the deposits is performed.

Summarizing above, the magnitude of the waveform changes depending on the thickness of the plate at the laser irradiation point, and by mapping the amplitude change and spectral peak change of the waveform, a distribution as shown in Fig. 1 (d) is obtained. By obtaining such a distribution in two dimensions, we believe that an image of the deposits under the laser irradiation area can be obtained.

Researches on SLS imaging done by one of the authors of the current paper showed that by using the wave field after diffusion, it is possible to image internal wall thinning even in complex geometries such as branching pipes, independent of the receiving position [19,21]. In addition, by using LDV and wireless microphones, damage imaging by remote measurement was realized [16,18,20]. Furthermore, imaging disturbance caused by high-speed laser scanning was analyzed in detail, and it was shown that spurious images can be reduced by using multiple receiving points [16].

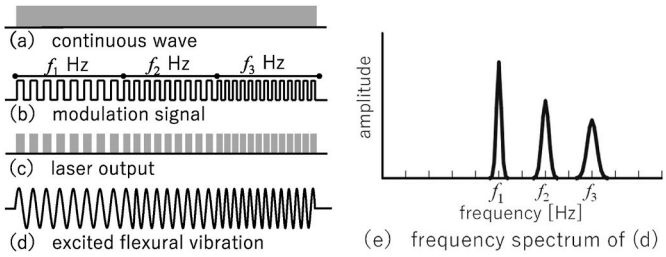

Fig. 2. Laser output, modulation signals, excited waveform and its frequency spectrum.

3. Experimental set-up and imaging procedure

3.1. Laser modulation

Generally, since a large pulse output is required to generate elastic waves, Q-switched YAG and CO_2 lasers have been used [24]. However, the use of such pulsed laser prevents us from controlling the frequency and waveform of the generated ultrasonic waves, and the broadband pulsed waves generated by the laser are generally small in the diffuse field. On the other hand, fiber lasers can now realize switching or amplitude modulation of laser output by external signals, making it possible to create arbitrary waveforms such as long-duration burst waves and chirp waves in the excitation of ultrasonic waves.

By employing a fiber laser for excitation of elastic waves, burst waves and chirped waves can be used. Narrowband burst waves generate resonances within the structure, and a diffuse field is not well formed, making it difficult to obtain a clear image in the SLS. On the other hand, chirp waves have a broader bandwidth, so the effect of resonance in the structure is reduced and a clearer image can be obtained. However, since we are considering a completely remote inspection using an LDV for receiving waveforms, the signal level of the elastic wave excited by the chirp wave may be insufficient.

Therefore, a previous study done by one of the authors presented that defect images can be acquired by excitation of elastic waves using a continuous wave laser modulated by an external modulation signal consisting of three different frequencies [17]. In this paper, we also used a fiber laser (Fujikura FLC-0300S, wavelength 1095 nm, maximum output power 300 W) that outputs a continuous wave and is modulated by an external signal to excite ultrasonic wave. The external modulation signal was a rectangular wave created by a digital-to-analog converter (NI, USB-6351). A schematic diagram of the laser output, the modulation signal provided, and the ultrasonic wave excited by the modulation signal are shown in Fig. 2. If no modulation signal is applied to the laser, a continuous wave shown in Fig. 2(a) is output, but when a rectangular signal with one period of $1/f_1$, $1/f_2$, and $1/f_3$ as shown in (b) is given as a modulation signal, a laser beam corresponding to it as shown in (c) is output. By irradiating the laser beam onto the material, elastic waves with a time interval roughly similar to the laser output are excited as shown in (d). In the experiments, the duty ratio of the modulation signal is 55 %, and therefore, the laser output becomes 165 W. As a result, at the frequency of f, $165/f$ J is the output energy of one laser shot. Since the frequency used is from 5 kHz to 29 kHz in this study, the output energy of one laser shot is from 5.7 mJ to 33 mJ. The elastic wave generated by the modulation laser is measured and Fourier transformed to obtain a frequency spectrum with peaks at f_1, f_2, and f_3 as shown in

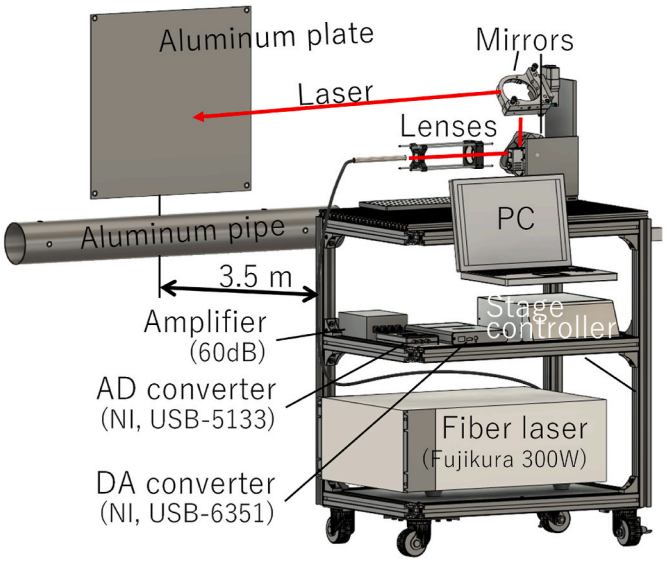

Fig. 3. Experimental system and specimens.

Fig. 2 (e). These frequency peaks are often easy to detect even when the time waveform is buried in noise. Therefore, although the use of a laser and a diffuse field in this method reduces the signal-to-noise ratio, the ultrasonic measurement method using such a laser modulation technique can significantly improve the signal-to-noise ratio, thereby enabling imaging of deposits.

3.2. Image enhancement with multiple frequencies and multiple receivers

In this study, two averaging methods are used to clarify images in an SLS, following [17]: the first is the averaging of images obtained at several frequency peaks when modulation signals with multiple frequencies as shown in Fig. 2 are used, and the second is the averaging of images obtained at multiple receiving positions.

The SLS images provides darker areas representing larger spectrum peaks due to the presence of thin damaged areas, while lighter areas represent smaller spectrum peaks due to intact areas. However, actual SLS images have spurious dark areas even at intact areas. Previous studies on the SLS imaging have demonstrated that this pattern originates from the resonance of the entire structure [11–20]. Since the pattern caused by the resonance varies depending on the frequency of the excited wave, in the previous study, ultrasonic waves of multiple frequencies were excited simultaneously by giving a modulation signal to the laser with three different frequencies connected in series, as shown in Fig. 2 (b). Since multiple peaks appear in the frequency spectrum obtained from the waveform of the ultrasonic wave excited in this way, as shown in Fig. 2(d), an average image was obtained from the average value of each frequency spectrum peaks [17]. In this study as well, an averaging method using multiple frequencies was used to reduce the influence of resonance patterns.

In basic experiments of this study, four piezoelectric disks with the diameter of 15 mm and resonant frequency of 6 kHz were used to measure the elastic waves on plates and pipes. When a piezoelectric disk is used as a security buzzer, it emits a sound at a resonant frequency of 6 kHz, but when attached to a metal material, it can detect vibrations up to about 100 kHz, covering the frequency band used in this study. The resonance pattern, signal level, and sensitivity of the sensor differ depending on the measurement position. Therefore, multiple piezoelectric disks were placed at multiple positions to measure the waveforms simultaneously at different positions. This allows us to acquire images at multiple positions, and a clearer image is stably obtained by averaging these images [17].

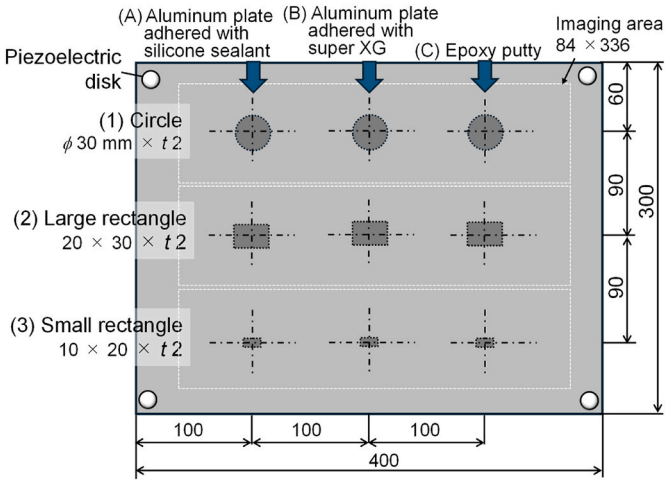

Fig. 4. Aluminum plate with bonded objects.

3.3. Experimental systems

Fig. 3 shows the experimental system used in this study. The distance between the specimen and the measurement system was about 3.5 m. The next section shows the results of the imaging experiment using a specimen with various kinds of deposits adhered on the back side of an aluminum plate, and Sect. 5 shows the results of detecting bonded objects on the inner surface of an aluminum pipe. As described in Sect. 3.1, the DA converter provided a modulation signal to irradiate a modulated laser beam onto the test object and to excite ultrasonic wave with a frequency matching the modulation signal. The modulation signals used in the experiments are described in detail in Sects. 4 and 5. The laser irradiation point was scanned two dimensionally on the surface of specimens by rotating two mirrors with rotation stages. The focal spot was set to be about 0.3 mm in diameter on the surface by adjusting the distance between the concave lens (f = -50) and convex lens (f = 200) located on the optical path before these mirrors. Strictly speaking, the spot diameter changes slightly because the distance from the convex lens changes depending on the laser irradiation position. However, the laser spot is sufficiently small at any scanning point compared to the wavelength of the Lamb wave generated on the plate, and therefore special calibration and adjustment of the spot diameter are not required. The scanning pitch was set, on the plane at the distance of 3.5 m from the experimental system, to Δx, Δy = 4 mm in the horizontal and vertical directions, respectively, but the scanning pitch was not the same distance on the pipe surface. At each point, a modulated laser beam was irradiated for 10 ms.

The waveform detected by the piezoelectric disks attached to the test object was amplified by 60 dB using an amplifier, and then stored to PC memory through an analog-to-digital converter (NI, USB-5133) for image processing. The waveforms measured by the LDV were directly captured by the AD converter and processed in the same manner. The waveforms were recorded for 20 ms after laser irradiation, filtered with a 1 kHz high-pass filter and an 80 kHz low-pass filter in the PC, and then subjected to a fast Fourier transform to obtain images using the methods described in Sects. 3.1 and 3.2. Since waveforms obtained vary greatly depending on the laser irradiation position, they are not shown here. References [14–18] may be useful.

4. Imaging results for a flat plate with deposits

First, in order to investigate the possibility of detecting deposits by an SLS and the effects of the size, shape, adhesion method, and frequency bandwidth used, we conducted experiments of imaging simulated deposits using a flat plate with an object attached to its back

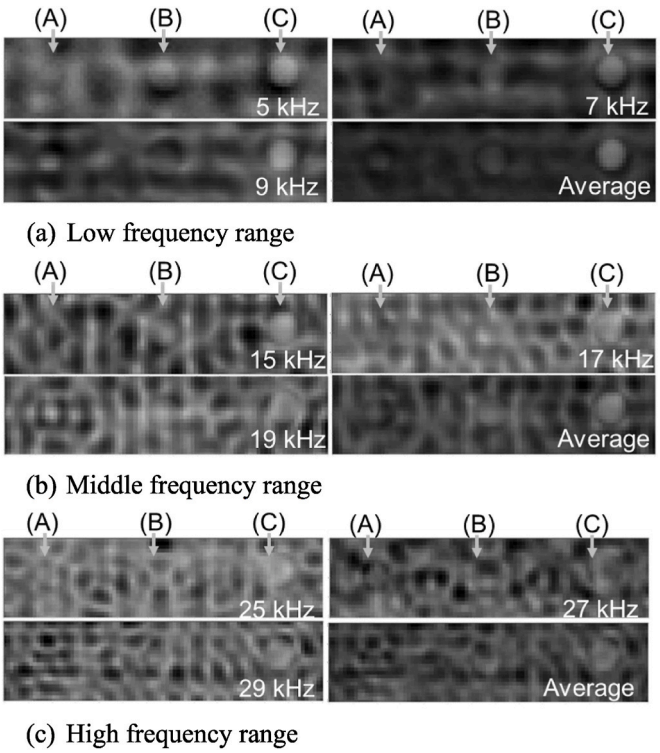

Fig. 5. Imaging results for circular bonded objects for various frequency ranges.

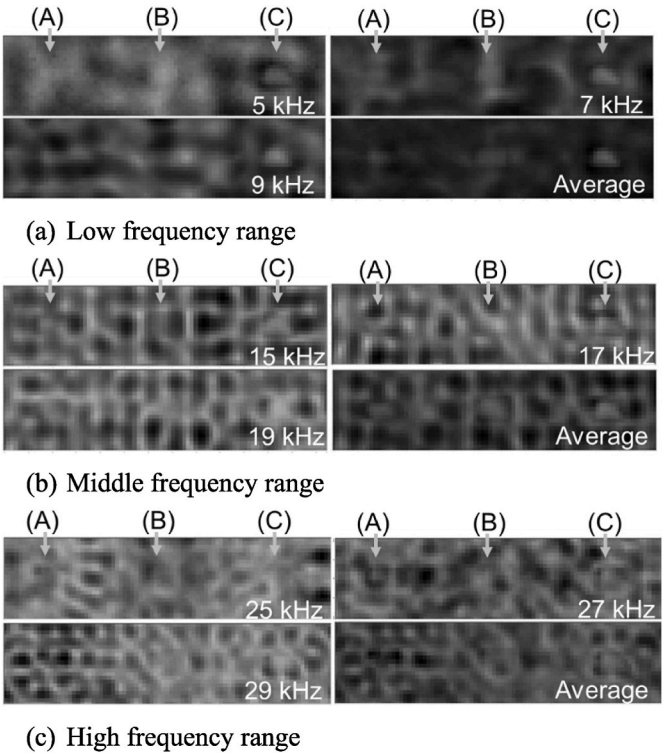

Fig. 6. Imaging results for large rectangular bonded objects for various frequency ranges.

surface. Fig. 4 shows a 300 mm × 400 mm × 3 mm aluminum plate used in the experiment. Four piezoelectric disks for measuring vibrations were attached to the four corners of the plate on the laser irradiated surface with vinyl tape. On the reverse side of the plate, opposite to the

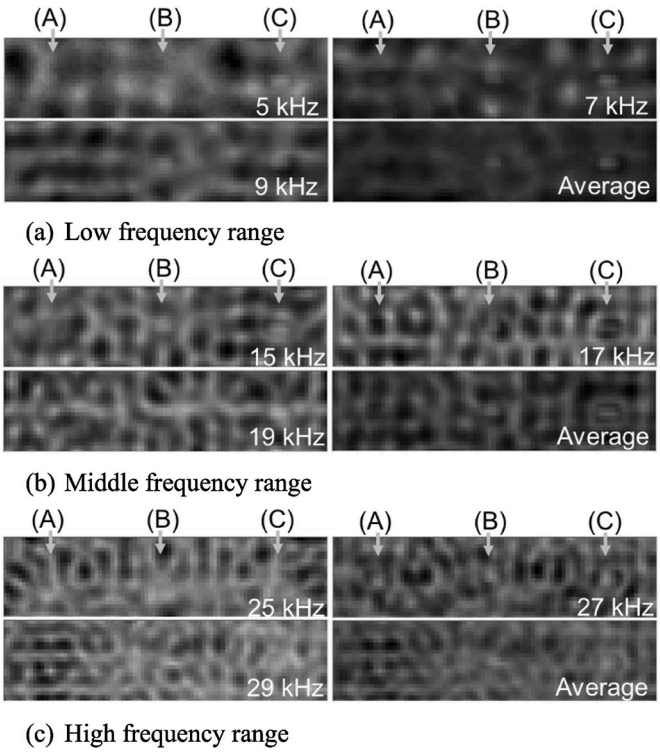

Fig. 7. Imaging results for small rectangular bonded objects for various frequency ranges.

laser irradiated surface, three different shapes of simulated deposits were attached in three different ways. As shown in Fig. 4, (1) circular plates (diameter 30 mm, thickness 2 mm), (2) large rectangular plates (20 mm × 30 mm × 2 mm), and (3) small rectangular plates (10 mm × 20 mm × 2 mm) are adhered from the top. In the left column (A), circular and rectangular aluminum plates of 2 mm thickness were bonded with a silicone sealant (Konishi Co., Ltd., Bath Bond Q #04891). This silicone sealant is usually used for repairing and filling bathtubs and metal pipes, and is used to fill gaps between adherends. Therefore, the adhesive itself has low rigidity. The center column (B) shows a similar example, in which circular and rectangular aluminum plates of 2 mm thickness are bonded with an acrylic modified silicone resin-based elastic adhesive (Cemedine Co., Ltd., SUPER XG AX-014). Generally, this adhesive is used where strong adhesion is required. In the rightmost column (C), epoxy putty (Cemedine Co., Ltd., HC-115) was molded into the same shape as the aluminum pieces in (A) and (B) and attached to an aluminum flat plate. This epoxy putty is often used to repair or fill in missing parts of materials, and it can be freely formed with two different clay-like materials in its initial state, and it becomes rigid like metal after drying by mixing these two materials. This specimen simulates (A) a softly bonded metal deposit, (B) a tightly bonded metal deposit, and (C) a rigid deposit that is hard to deform.

Three areas of 84 mm × 336 mm, indicated by the white dashed lines in Fig. 4, were irradiated with lasers at a scan pitch of Δx, $\Delta y = 4$ mm to image the bonded objects according to the method described in Sect. 3. For each area, an external modulation signal of three frequencies was applied for 10 ms (3.3 ms per frequency) within the frequency range of the amplifier used, in (a) the low frequency range (5, 7, 9 kHz), (b) the medium frequency range (15, 17, 19 kHz), and (c) the high frequency range (25, 27, 29 kHz), respectively. Figs. 5–7 show the results for (1) circular bonded objects, (2) large rectangular bonded objects, and (3) small rectangular objects, respectively.

Since the images with one frequency each (upper left, upper right, and lower left) may not give a correct trend due to the influence of the resonance of the whole structure at that frequency, we will focus on the

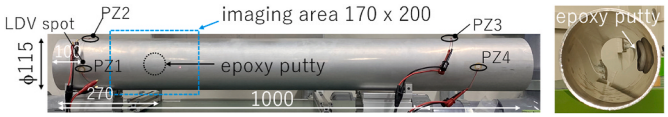

Fig. 8. Aluminum pipe and a bonded object.

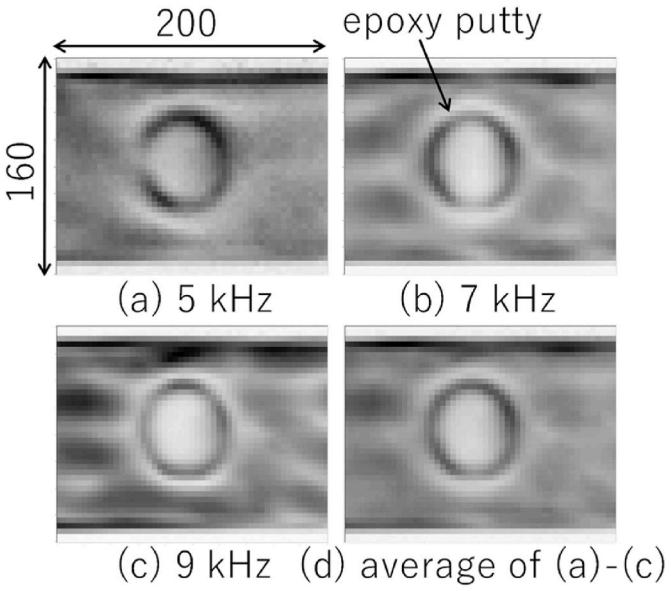

Fig. 9. Images created by the signals only at PZ1.

lower right figure, which is the average of these three images. First, in the case of the 30 mm diameter circular deposits shown in Fig. 5, we can see the circular images become clearer in the order of (C), (B), and (A). The circular area is white, which indicates that the bending vibration generated by the laser irradiation is suppressed due to the bonded objects. The fact that almost no image was obtained in the case of bonding with the silicone sealant in (A) indicates that the silicone sealant was soft even after curing and had little effect on the deformation caused by the laser irradiation. The same tendency is observed in Figs. 6 and 7. Comparing the average images in Figs. 5–7 and examining the frequency band, the clearest image of the bonded objects was obtained in the low-frequency band in (a). As shown in Sect. 3.2, the resonance pattern of the entire structure is reduced by using multiple receiver locations and frequencies, but it is still considered to have a larger effect than the small changes in the bending vibration due to the bonded objects. Especially when the resonance pattern is as large as the size of the objects (e.g. (b) and (c) in Fig. 7), it was impossible to obtain images of the bonded objects.

When the bonded objects were obtained as an image, for example, in the averaged images shown in Fig. 5 (a) and 6 (a), a black contour indicating higher vibration energy is shown around the white area representing the bonded objects. This is due to the fact that, as shown in Ref. [15], reflections from the edge surfaces of the bonded objects occur and the evanescent modes are superimposed, resulting in an increase in vibration energy. This contour tends to be easier to recognize the larger the size of the deposit, which can be seen in the comparison between Figs. 5 and 7.

5. Imaging of an object attached on the inner surface of a pipe

5.1. Experiments with piezoelectric disks

This section shows the imaging results of an aluminum pipe with an object attached to its interior, as shown in Fig. 8. The dimensions of the

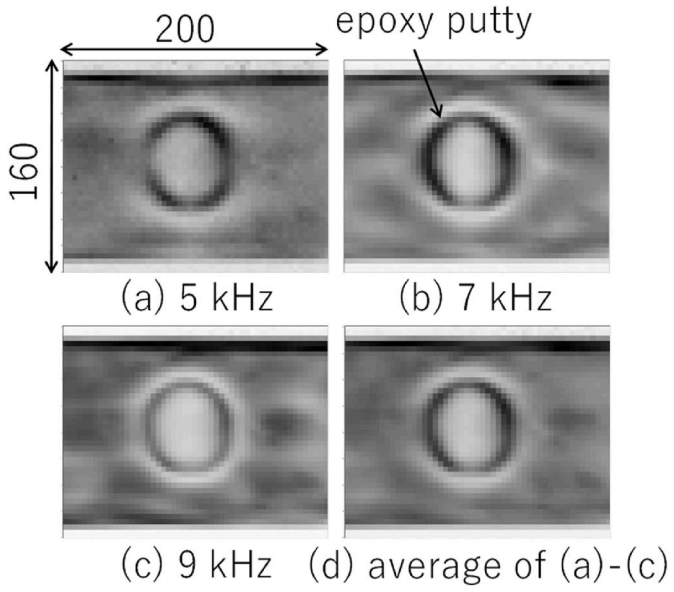

Fig. 10. Images created by the signals at four positions, PZ1 – PZ4.

specimen are 115 mm in outer diameter, 1000 mm in length, and 3 mm in thickness, with the object attached at approximately 270 mm from the left end. Epoxy putty, which was used in Sect. 4, was employed as the object attached to the inner surface of the pipe. The epoxy putty was a circular disk with a diameter of approximately 50 mm and a thickness of approximately 10 mm. Piezoelectric disks were attached to the surface of the specimen at four locations as shown in Fig. 8, and an imaging area was 170 mm × 200 mm in the experiments. The imaging experiments were performed with the laser modulated at low frequencies (5, 7, and 9 kHz), which were relatively good results obtained in the experiments with the flat plate described in the previous section. In the case of such curved surfaces as pipes, the laser spot size varies significantly depending on the laser irradiation position, but in most areas the spot size is sufficiently smaller than the wavelength of the generated guided wave. Therefore, the effect of the difference in spot size on the image is small. For example, in Ref. [16], images are obtained appropriately even if the wall thinning in the pipe is at various circumferential positions.

Figs. 9 and 10 show the experimental results: Fig. 9 is the image obtained using only the waveform received by the piezo disk at PZ1 in Figs. 8 and 10 is the result of averaging the waveforms at the four locations from PZ1 to PZ4. The images (a)-(c) are obtained by plotting the values of the frequency peaks at 5 kHz, 7 kHz, and 9 kHz, respectively, and (d) is the average of these images.

The image in Fig. 10, which is averaged over four points, is slightly clearer, but all of them are white at the location of the bonded object, indicating that the vibration energy is low, which shows that the bonded object is properly imaged. In addition, the overall resonance pattern can be seen at locations other than the object. For example, in the image in Fig. 9 (c), two black bands are seen to the left of the circular adhesion, and this periodic pattern represents the resonance of the entire structure. Lines also appear at the upper end of the pipe, indicating an overall resonance pattern, which was obtained in the previous paper for pipes [16]. As in the flat plate case, there are also black outlines of the circular object, which also indicates the areas of increased energy due to interaction with the evanescent mode.

5.2. Experiments with a laser Doppler vibrometer

In the decommissioning site, we cannot usually get close to the object to be inspected due to radiation. Therefore, it is desirable to be able to remotely measure the ultrasonic waves excited by laser irradiation. The LDV (Polytec, OFV-5000) was placed right next to the laser excitation

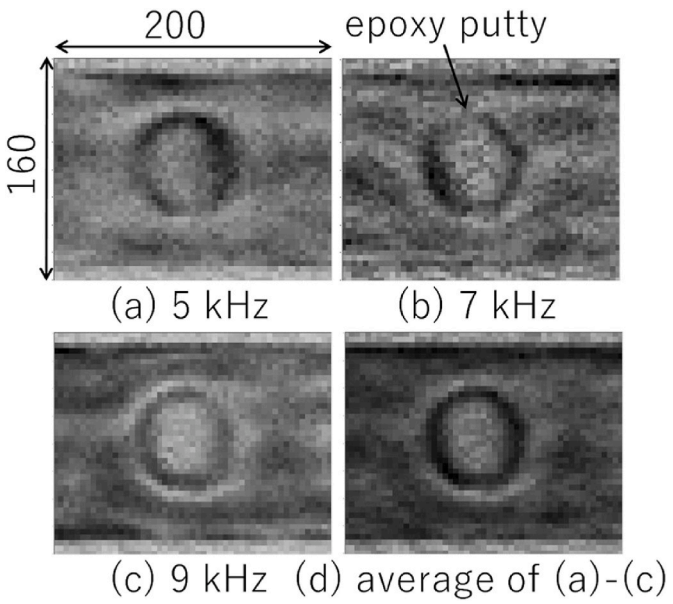

Fig. 11. Images with LDV

device at a distance of about 3.5 m from the specimen. Fig. 11 shows the distribution plots of the frequency peaks at 5 kHz, 7 kHz, and 9 kHz as in Figs. 9 and 10, and (d) is the average of these peaks. Compared with Fig. 9, the signal-to-noise ratio of the LDV signal is lower than that of the piezoelectric signal, and although the image is blurred, the position, shape, and size of the bonded object can be generally captured. The laboratory tests at a distance of about 3.5 m represents that bonded objects in a pipe can be detected by the non-contact manner of an SLS.

6. Conclusions

This study presented the experimental results to apply an SLS imaging method to the detection of deposits inside pipes, which is required for the decommissioning of the Fukushima nuclear power plant. First, ultrasonic measurements were performed on a test specimen with a bonded object attached to the back of a flat plate using an SLS with piezoelectric disks as the receivers. The results showed that the image of the bonded object was clear for strong adhesion, but the smaller the size and the weaker the strength of adhesion, the blurrier the image became, as expected. It was also shown that bonded objects inside the pipe could be detected by the same experimental system. Furthermore, when LDV was used to measure ultrasonic waves, images of bonded objects were obtained appropriately, although some degradation of images was observed due to a lower signal-to-noise ratio. In the future, it is necessary to evaluate the effectiveness of this method for the size and strength of bonded objects expected in decommissioning process.

CRediT authorship contribution statement

Shoma Tanaka: Writing – original draft, Validation, Investigation, Data curation, Methodology. **Takahiro Hayashi:** Writing – review & editing, Validation, Supervision, Project administration, Methodology, Investigation, Funding acquisition, Formal analysis, Data curation, Conceptualization, Software. **Naoki Mori:** Writing – review & editing, Validation, Methodology, Investigation, Data curation.

Declaration of competing interest

The authors declare the following financial interests/personal relationships which may be considered as potential competing interestsTakahiro Hayashi reports financial support was provided by Japan Atomic Energy Agency. If there are other authors, they declare that they have no known competing financial interests or personal relationships that could have appeared to influence the work reported in this paper.

Data availability

The data that has been used is confidential.

Acknowledgement

This work was supported by JAEA Nuclear Energy S&T and Human Resource Development Project through concentrating wisdom Grant Number JPJA23P23813810.

References

[1] M. Palaniappan, R. Subbaratnam, A. Baskaran, R. Chandramohan, The role of non-destructive examination in improving the quality for pipeline and pressure vessels - case studies, Int. J. Pres. Ves. Pip. 73 (1997) 33–37, https://doi.org/10.1016/S0308-0161(97)00031-8.
[2] H.A. Kishawy, H.A. Gabbar, Review of pipeline integrity management practices, Int. J. Pres. Ves. Pip. 87 (2010) 373–380, https://doi.org/10.1016/j.ijpvp.2010.04.003.
[3] J.L. Rose, A baseline and vision of ultrasonic guided wave inspection potential, J. Pressure Vessel Technol. 124 (2002) 273–282, https://doi.org/10.1115/1.1491272.
[4] J.L. Rose, Ultrasonic Guided Waves in Solid Media, Cambridge University Press, 2014, https://doi.org/10.1017/CBO9781107273610.
[5] D.N. Alleyne, B. Pavlakovic, M.J.S. Lowe, P. Cawley, Rapid long-range inspection of chemical plant pipework using guided waves, Insight 43 (2001) 93–96, 101.
[6] P. Cawley, M.J.S. Lowe, D.N. Alleyne, B. Pavlakovic, P. Wilcox, Practical long range guided wave testing: applications to pipes and rails, Mater. Eval. 61 (2003) 66–74.
[7] P.J. Mudge, Field application of the Teletest (R) long-range ultrasonic testing technique, Insight 43 (2001) 74–77, http://ubumexico.centro.org.mx/text/emr/articles/mumma_liveelectronic.pdf\npapers3://publication/uuid/D4D8FBA3-C0A6-4214-8B30-44C6697DC04D.
[8] T. Hayashi, K. Kawashima, Z. Sun, J.L.J.L. Rose, Analysis of flexural mode focusing by a semianalytical finite element method, J. Acoust. Soc. Am. 113 (2003) 1241–1248, https://doi.org/10.1121/1.1543931.
[9] T. Hayashi, M. Murase, Defect imaging with guided waves in a pipe, J. Acoust. Soc. Am. 117 (2005) 2134–2140, https://doi.org/10.1121/1.1862572.
[10] T. Hayashi, M. Nagao, M. Murase, Defect imaging with guided waves propagating in a long range, Transactions of the Japan Society of Mechanical Engineers Series A 72 (2006) 1941–1948, https://doi.org/10.1299/kikaia.72.1941.
[11] T. Hayashi, M. Murase, M.N. Salim, Rapid thickness measurements using guided waves from a scanning laser source, J. Acoust. Soc. Am. 126 (2009) 1101–1106, https://doi.org/10.1121/1.3177268.
[12] T. Hayashi, M. Murase, T. Kitayama, Frequency dependence of images in scanning laser source technique for a plate, Ultrasonics 52 (2012) 636–642, https://doi.org/10.1016/j.ultras.2012.01.003.
[13] T. Hayashi, M. Murase, N. Ogura, T. Kitayama, Imaging defects in a plate with full non-contact scanning laser source technique, Mater. Trans. 55 (2014) 1045–1050, https://doi.org/10.2320/matertrans.I-M2014817.
[14] T. Hayashi, Imaging defects in a plate with complex geometries, Appl. Phys. Lett. 108 (2016) 081901, https://doi.org/10.1063/1.4942599.
[15] T. Hayashi, M. Fukuyama, Vibration energy analysis of a plate for defect imaging with a scanning laser source technique, J. Acoust. Soc. Am. 140 (2016) 2427–2436, https://doi.org/10.1121/1.4964275.
[16] T. Hayashi, Non-contact imaging of pipe thinning using elastic guided waves generated and detected by lasers, Int. J. Pres. Ves. Pip. 153 (2017) 26–31, https://doi.org/10.1016/j.ijpvp.2017.05.006.
[17] T. Hayashi, High-speed non-contact defect imaging for a plate-like structure, NDT E Int. 85 (2017) 53–62, https://doi.org/10.1016/j.ndteint.2016.10.009.
[18] T. Hayashi, Defect imaging for plate-like structures using diffuse field, J. Acoust. Soc. Am. 143 (2018), https://doi.org/10.1121/1.5030915.
[19] A. Maeda, T. Hayashi, Defect imaging from a remote distance by using scanning laser source technique with acoustic microphones, Mater. Trans. 59 (2018), https://doi.org/10.2320/matertrans.M2017326.
[20] S. Nakao, T. Hayashi, Non-contact imaging for delamination using diffuse field concept, Jpn. J. Appl. Phys. 58 (2019), https://doi.org/10.7567/1347-4065/ab0ada.
[21] International Atomic Energy Agency, The Fukushima Daiichi Accident, International Atomic Energy Agency, 2015.
[22] Nuclear Damage Compensation and Decommissioning Facilitation Corporation, Technical Strategic Plan 2023for Decommissioning of the Fukushima Daiichi Nuclear Power Station of Tokyo Electric Power Company Holdings, Inc., 2023. https://dd-ndf.s2.kuroco-edge.jp/files/user/pdf/en/strategic-plan/book/20231222_SP2023eFT.pdf. (Accessed 5 March 2024).
[23] C.B. Scruby, Some applications of laser ultrasound, Ultrasonics 27 (1989) 195–209.

[24] C.B. Scruby, L.E. Drain, Laser Ultrasonics: Techniques and Applications, CRC Press, 1990.
[25] S. Krishnaswamy, Theory and applications of laser-ultrasonic techniques, in: Ultrasonic Nondestructive Evaluation, CRC Press, 2003, pp. 435–494, https://doi.org/10.1201/9780203501962.ch7.
[26] D.A. Hutchins, K. Lundgren, S.B. Palmer, A laser study of transient Lamb waves in thin materials, J. Acoust. Soc. Am. 85 (1988) 1441–1448, https://doi.org/10.1121/1.397981.